Probing the thermoelectric transport properties of n-type Bi_2Te_3 close to the limit of constitutional undercooling*

Feng Song-Ke(冯松科), Li Shuang-Ming(李双明)†, and Fu Heng-Zhi(傅恒志)

State Key Laboratory of Solidification Processing, Northwestern Polytechnical University, Xi'an 710072, *China*

(Received 10 July 2014; revised manuscript received 7 August 2014; published online 21 October 2014)

Bulk n-type Bi_2Te_3 single crystals with optimized chemical composition were successfully prepared by a high temperature-gradient directional solidification method. We investigate the influence of alloy microstructure, chemical composition, and growth orientation on the thermoelectric transport properties. The results show that the composition of single-crystal Bi_2Te_3 alloy, along the *c* axis direction, could be slightly tuned by changing the growth rate of the crystal. At a rate of 18 mm/h, the formed Bi_2Te_3 crystal exhibits good thermoelectric properties. At 300 K, a maximum Seebeck coefficient of -245 μV/K and an electrical conductivity of 5.6×10^4 S/m are acquired. The optimal power factor is obtained as 3.3×10^{-3} W/K^{2}m, with a figure of merit of 0.74. It can be attributed to the increased tellurium allocation in the Bi_2Te_3 alloys, as verified well by the density functional theory calculations.

Keywords: thermoelectric property, directional solidification, Bi_2Te_3, density functional theory

PACS: 72.15.jf, 81.30.Fb, 74.25.F–, 32.10.Dk **DOI:** 10.1088/1674-1056/23/11/117202

1. Introduction

Bismuth telluride crystal, a new three-dimensional (3D) topological insulator, has raised great research interest in the field of fault-tolerant quantum computing, high-temperature spintronic devices, and engineering thermoelectric applications as the best candidate material.[1–6] Their thermoelectric performance is defined by a dimensionless figure of merit $ZT = (S^2\sigma)T/k$, where σ is the electrical conductivity, S is the Seebeck coefficient, and k is the thermal conductivity. The power factor (PF), $S^2\sigma$, expresses a comprehensive transport property of thermoelectric materials. To increase the magnitude of ZT, one needs to improve PF or reduce thermal conductivity of the material. Working in both ways would be better.

The value of ZT for bulk Bi_2Te_3 alloys is mainly dependent on microstructures and element distribution in the alloys.[7,8] Polycrystalline microstructures without any preferred orientations will induce inner Seebeck effect and electric cycles, leading to a decrease in the thermoelectric transport property.[9] This undesirable effect has been revealed in Bi_2Te_3 compounds prepared by spark plasma sintering (SPS)[10,11] and hot pressed sintering.[12,13] The element distribution change of Bi and Te in the crystal can cause variations in conductive type and carrier concentration, resulting in non-uniform thermoelectric performance of the material.[14–18] A single crystal with preferred orientation and optimized chemical composition is most beneficial to the performance of the alloy. Fleurial *et al.*[19] carried out a research on the relationship between the thermoelectric properties and carrier concentration of the Bi_2Te_3 alloys at room temperature, not involving the practical temperature section of the thermoelectric power generation ranging from 300 K to 500 K.[20] Shen *et al.*[10] and Nassary *et al.*[14] have shown the temperature-dependent thermoelectric properties of the Bi_2Te_3 alloys, without details concerning the elemental distribution in the crystal. These phenomena were also observed in our previous directionally grown Bi_2Te_3 polycrystals.[18] In view of this, the relationship between concentration allocation, as well as the temperature profile, and thermoelectric properties of the large bulk Bi_2Te_3crystal prepared under high-temperature gradients remains lacking, to our best knowledge.

In this study, a modified zone melting method with a high thermal gradient ($G_L = 178$ K/cm) is employed to grow bulk Bi_2Te_3 single crystals. The thermoelectric performance change caused by the variation of the chemical concentration and preferred orientations of the grown Bi_2Te_3 crystals was investigated from 300 K to 520 K. It is noted here that the studied n-type Bi_2Te_3 alloys are cooled close to the limit of constitutional undercooling. The first-principle calculations based on the density functional theory (DFT) are utilized to obtain the transport thermoelectric coefficient and the computed results are compared with the experimental data.

2. Methods and theory

2.1. Material methods

N-type bismuth telluride ingot was prepared from high purity (99.999%) bismuth and tellurium granules in a vacuum furnace. The as-cast rods with a diameter of 13 mm were cut into a length of 90 mm, sealed in high pure quartz pipes with

*Project supported by the National Natural Science Foundation of China (Grant No. 51074127) and the Research Fund of the State Key Laboratory of Solidification Processing of Northwestern Polytechnical University, China (Grant No. SKLSP201010).

†Corresponding author. E-mail: lsm@nwpu.edu.cn

© 2014 Chinese Physical Society and IOP Publishing Ltd

150 mm in height and 14 mm in inner diameter. The pipe containing rod was melted under 2.3×10^{-3} Pa in a modified zone melting furnace (see Fig. 1). The growth rates in the directional solidification were set to 3.5 mm/h and 18 mm/h. The measured temperature gradient was about 178 K/cm.

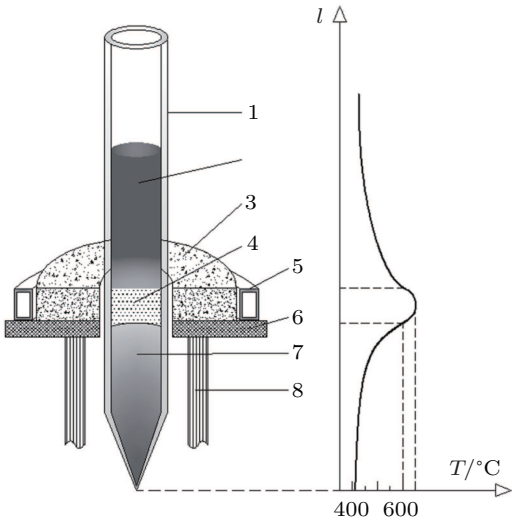


Fig. 1. Crystal growth by the zone melting method with the temperature profile. 1, silica crucible; 2, raw material; 3, graphite heater; 4, molten alloy; 5, induction heating coil; 6, boron nitride baffle; 7, growth crystal; 8, holder.

Phases and lattice constants in the solidified samples were identified on a DX-2700 X-ray diffractometer, using a Cu X-ray tube (Kα) with a range of 15°–75° and a step size of 0.02°. The microstructure and chemical compositions of the grown Bi_2Te_3 samples were examined by SEM (VEGA II LMH) and ICP (IRIS ER/S), respectively. The thermal conductivity along the cleavage plane of the Bi_2Te_3 crystal was measured on a laser flash apparatus (LFA 457 NETZSCH). The Hall coefficient along the cleavage plane was measured at 292 K by applying a magnetic field of 1.0 T perpendicular to the c axis, and the carrier concentrations and mobility were obtained by using the Hall coefficient and electrical resistivity. Along the cleavage plane of the grown Bi_2Te_3 samples, the Seebeck coefficient and electrical resistivity were measured using a ZEM-3(M8) (ULVAC-RIKO) apparatus at temperatures ranging from 300 K to 520 K. The thermoelectric figure of merit ZT was evaluated from the above measured results.

To reveal the optimized structure and transport coefficients of the crystal, the first-principle calculations were performed using the Quantum-ESPRESSO package[21] within the density functional theory (DFT) by means of a planewave pseudopotential method. The generalized gradient approximation of the Perdew–Burke–Ernzerho (PBE)[22] was applied to evaluate the exchange–correlation energy. The ultrasoft pseudopotentials[23] for both Te and Bi were taken for electron–ion interaction in pseudo atomic calculation, with spin–orbit coupling being included. In this study, the kinetic cut-off energy was 45 Ry. An $8 \times 8 \times 8$ Monkhorst-pack k-point sampling was used in the irreducible wedge of Brillouin zone for the crystal relaxation. The crystal structure was relaxed by the BFGS[24] method for both lattice parameters and atomic internal coordinates until the stress along each lattice direction was less than 0.02 Kbar. For the transport calculation, the optimized Bi_2Te_3 structure was applied for the calculation of the band structures with a $54 \times 54 \times 54$ denser grid. The obtained band energy is brought to the BoltZTraP package[25] to calculate the transport coefficients.

2.2. Constitutional undercooling criterion

A high-quality single crystal can be prepared by maintaining a stable planar solid/liquid interface during its directional solidification. In the case of the Bi_2Te_3 alloy, the advancing planar interface will break out at the onset of the constitutional undercooling. According to the criterion of constitutional undercooling,[26] the critical growth rate required for keeping a stable planner interface in directional solidification can be expressed as

$$v_c = \frac{GD_l k_0}{m(1-k_0)C_0} = \frac{GD_l}{m\Delta C_0}, \tag{1}$$

where G, D_l, k_0, m, and C_0 are the temperature gradient, liquid diffusion coefficient, equilibrium distribution coefficient, slope of the solid line, and initial alloy composition, respectively. By introducing the Bi–Te alloy phase diagram,[7] the parameters m and ΔC_0 were calculated as -0.441% and 7.936 wt.%, respectively. For the molten metal, the value of D_l is close to 1×10^{-9} m^2/s.[27] Substituting these values into Eq. (1), the critical growth rate for the stable growth of the planar interface was estimated to be 20 mm/h, higher than the controlled experimental growth rates, i.e., 3.5 mm/h and 18 mm/h. A stable grown planar interface should be observed in the directional solidification of the Bi_2Te_3 crystal.

3. Results and discussion

3.1. Microstructures

Directionally solidified microstructures of the Bi_2Te_3 crystal and their corresponding bulk X-ray spectra at the growth rates of 3.5 mm/h and 18 mm/h are shown in Fig. 2. The obtained crystals grew following preferred {001}-type lattice planes, corresponding to the c axis of the crystal. It means that the cleavage plane of the crystal is parallel to the growth direction, in agreement with the reported results of Nassary *et al.*[12] and Ainsworth *et al.*[21]

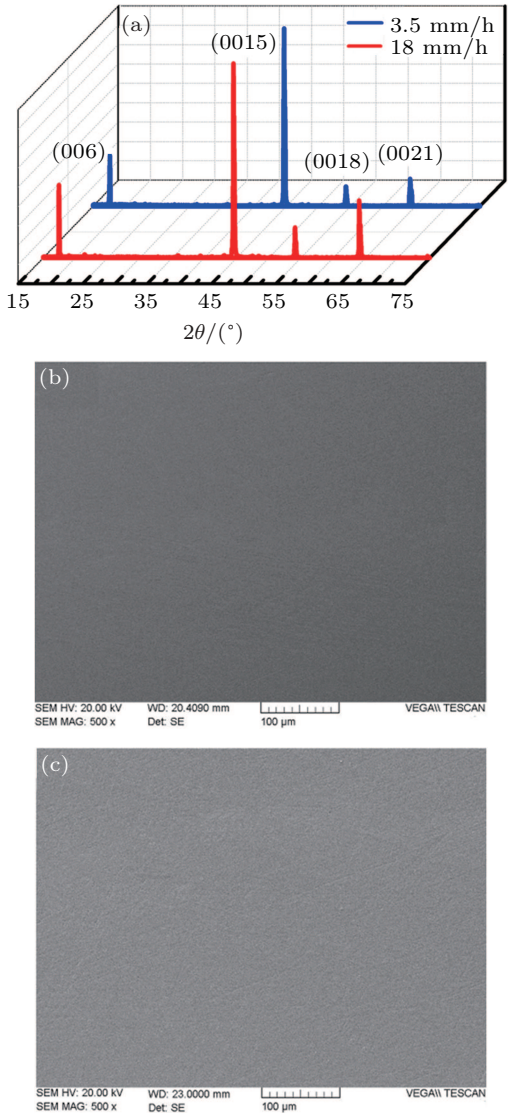


Fig. 2. (color online) (a) Bulk X-ray data of the grown Bi_2Te_3 crystals at different growth rates, and their microstructures of the transverse section at the growth rates of 3.5 mm/h (b) and 18 mm/h (c).

Planar interface microstructures could be observed in Figs. 2(b) and 2(c). It indicates that a single crystal growth pattern was acquired at both growth rates, correlating with the requirement of the constitutional undercooling criterion. No cracks were produced in the crystals during the directional solidification. At the growth rate of 18 mm/h, the growth efficiency of the single crystal can be improved by one order of magnitude than the previously reported growing methods.[14,28] A higher growth rate can be efficient to reduce the distance of the initial transition region for the establishment of a steady-state growth condition, improving the utilization efficiency of the Bi and Te raw materials.

The solidified phase and lattice constants of the crystals under the high-temperature gradient directional solidification were analyzed by XRD (see Fig. 3). It clearly shows that only Bi_2Te_3 phase formed in the directional solidification. With the growth rate increasing from 3.5 mm/h to 18 mm/h, the peaks shift 0.04°–0.05° to the right, as shown in the inner part of Fig. 3. This shifting means a reduction in the lattice constants of the crystal. Table 1 illustrates the change in lattice constants of the crystal. Both a and c become smaller with increasing growth rate. It can be attributed to the chemical composition variation. That is, Bi atoms were replaced by smaller Te atoms.

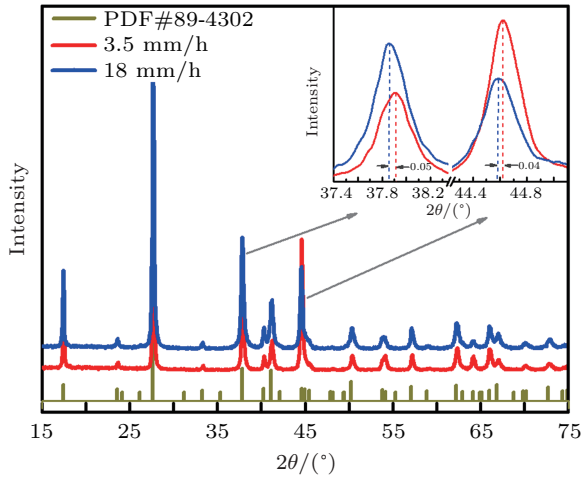


Fig. 3. (color online) Power X-ray data of the Bi_2Te_3 crystals at the growth rates of 3.5 mm/h and 18 mm/h.

Table 1. Chemical composition and lattice constants of the directionally solidified Bi_2Te_3 crystal at the growth rates of 3.5 mm/h and 18 mm/h. The first row data was calculated using the first-principle calculation.

Growth rate/mm·h^{-1}	Atomic percentage/at.%		Lattice constants/Å		
	Bi	Te	a	b	c
–	40.00	60.00	4.2944	4.2944	29.8623
3.5	39.88	60.12	4.3851	4.3851	30.6058
18	39.74	60.26	4.3751	4.3751	30.4113

This variation happens during the solidification process. Based on the crystal growth theory,[29] as long as a crystal growth process reaches a steady-state condition, the solid chemical composition at interface, C_s^*, can be expressed as

$$C_s^* = k_E C_0 = \frac{k_0 C_0}{k_0 + (1 - k_0)\exp(-v\delta_n/D)}, \tag{2}$$

where k_E is the effective distribution coefficient and δ_n is the thickness of melt boundary layer. As seen in Eq. (2), the solid concentration, C_s^*, approximates the melt composition, C_0, with increasing growth rate, where the chemical composition, C_0, is marked in Fig. 4 using dashed line in the binary Bi–Te phase diagram.[7] The composition of the Bi_2Te_3 crystal at 3.5 mm/h is 60.12 at.% Te–Bi. At 18 mm/h, it is 60.26 at.% Te–Bi, closer to the melt composition of C_0 (60.5 at.% Te–Bi). It is clear that the chemical composition of the single crystal was varied by changing the growth rate. In our case, this minor composition variation has caused a remarkable change in the transport property of the crystal.

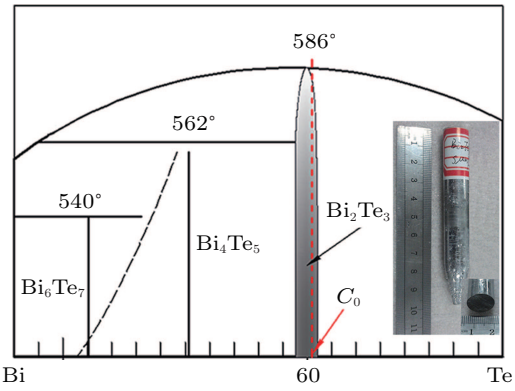


Fig. 4. (color online) Binary Bi–Te alloy phase diagram[7] and the initial chemical composition C_0.

3.2. Thermoelectric properties

3.2.1. Electronic transport property and Hall coefficient

The electrical conductivities of the solidified Bi_2Te_3 alloys increase with temperature (see Fig. 5). The electrical conductivity of the crystal solidified at 18 mm/h is larger than that at 3.5 mm/h. The lowest value reaches 5.6×10^4 S/m for the crystal grown at 18 mm/h, presenting a good boosting electronic transport property at room temperature.

Hall coefficient, R_H, is another important parameter to represent the transport properties of the material. To correctly measure the Hall coefficient, we took fore probes on the sample with a low-voltage alternating current parallel to the cleavage plane and using a magnetic field perpendicular to the cleavage plane. The results are listed in Table 2. The Hall coefficient of the grown crystals decreases with the growth rate from 3.5 mm/h to 18 mm/h. Simultaneously the carrier concentration n and carrier mobility μ_H can be obtained using $R_H = A_H/ne$ and $\mu_H = R_H\sigma$,[8] respectively. As shown in Table 2, the carrier concentration n of the grown Bi_2Te_3 crystal increases with the elevating growth rates, corresponding to the data of electrical conductivity at 300 K in Fig. 5. The carrier mobility of the grown crystals slightly drops with the growth rate, agreeing well with the results of Scherrer *et al.*[30] and Fleurial *et al.*[19] It means that the electronic transport properties of the crystals, i.e., the electrical conductivity ($\sigma = ne\mu_H$) and electronic thermal conductivity, are mainly dependent on the carrier concentration.

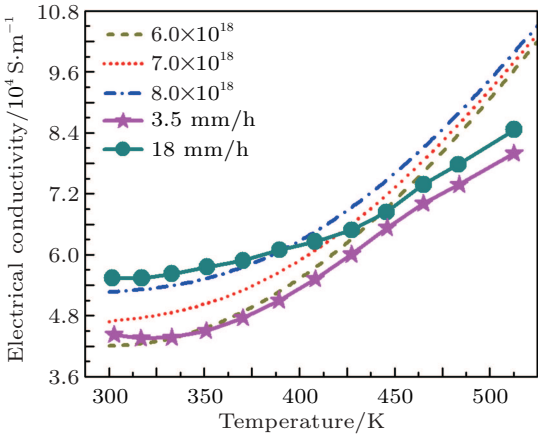


Fig. 5. (color online) Temperature dependence of electrical conductivity for Bi_2Te_3 crystals with the experimental data (solid lines) and theoretical calculations (dash lines).

It should be noted that different measurement methods can result in different Hall coefficient and make great deviation of the carrier concentration. Compared with the carrier mobility (μ_H), the carrier concentration (n) has a significant impact on the electrical conductivity of the Bi_2Te_3 material. To clearly illustrate the effect of carrier concentration on the transport properties of Bi_2Te_3 material, we use the first-principle calculation coupling with the semi-empirical Boltzmann equation to illustrate the effect of the varying charge carrier density on the electronic transport properties. All the transport properties were calculated along the cleavage plane in the Bi_2Te_3 crystal and the experimental results were also measured along this plane. The theoretical calculation data are given in Fig. 5 by dashed lines. The electrical conductivities of the Bi_2Te_3 alloy became large with increasing temperature and electronic concentration. The electronic concentration of the crystal grown at 18 mm/h is over 8.0×10^{18} cm^{-3}, larger than the crystal grown at 3.5 mm/h with the value of 6.0×10^{18} cm^{-3}. It can be attributed to the excess Te distribution in the Bi_2Te_3 alloy, as shown in Table 1. This phenomenon suggests that the electrical conductivity of the Bi_2Te_3 crystal can be uplifted by adjusting the growth rate to reallocate the chemical composition of the alloy.

Table 2. Experimental data of the Hall coefficient, electrical conductivity, carrier concentration, and carrier mobility of the directionally solidified n-type Bi_2Te_3 samples were measured at 295 K.

Experiment group	Type	Electrical conductivity/S·m^{-1}	Hall coefficient/cm^3·C^{-1}	Carrier concentration/cm^{-3}	Carrier mobility/cm^2·V^{-1}·S^{-1}
3.5 mm/h	n	4.40×10^4	−0.56	5.55×10^{18}	242
18 mm/h	n	5.49×10^4	−0.38	8.16×10^{18}	210
Rowe [a)]	n	5.58×10^4	−0.52	7.00×10^{18}	227
Scherrer [b)]	n	1.00×10^5	–	–	212
Fleurial [c)]	n	–	–	9.0×10^{18}	240

[a)] Ref. [7]. [b)] Ref. [30]. [c)] Ref. [19].

The theoretical calculations do not fit the experimental data at the temperature over 400 K. This can be explained in two reasons. First, more electrons are excited to the conduction bands at higher temperature in the Bi_2Te_3 crystal,[6] leading to increased carrier concentration and steeply raised electrical conductivity. This can also be observed in Si,[31] SiGe,[32] and PbTe[33] semiconductors. Second, the inner parameters of the relaxing time, electronic group velocity, and Fermi distribution function change nonlinearly with the temperature.[34] This also contributes to the departure of the calculation results from the experimental data. Even so, a good agreement has been achieved for the electrical conductivity for the Bi_2Te_3 crystal at temperature ranging from 300 K to 400 K.

3.2.2. Seebeck coefficient

The Seebeck coefficient is a key parameter for the thermoelectric material. The data of the measured temperature-dependent Seebeck coefficient in the directionally solidified Bi_2Te_3 crystals are shown in Fig. 6. It indicates that the absolute values of Seebeck coefficient of the grown crystals dropped monotonously with increasing temperature from 300 K to 500 K. The values for the crystal grown at 18 mm/h are larger than those at 3.5 mm/h. We fitted the experimental data with an approximate expression: $S = m_s(T - 300) - 250$ (m_s is equal to 0.75 for $T < 440$ K and 0.16 for $T > 440$ K). This implies that the Seebeck coefficient of the crystals drops slowly as the temperature is above 440 K.

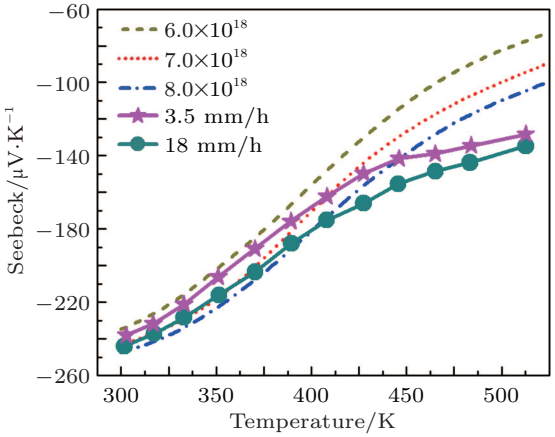


Fig. 6. (color online) Temperature dependence of Seebeck coefficients for the Bi_2Te_3 crystals with the experimental data (solid lines) and theoretical calculations (dash lines).

As shown in Fig. 6, the maximum Seebeck coefficient, −246 μV/K, was obtained for the Bi_2Te_3 crystal grown at 18 mm/h during the directional solidification, close to the previously reported value of −250 μV/K.[19] At 500 K, the lowest Seebeck coefficient of the Bi_2Te_3 crystal grown at 18 mm/h can reach −130 μV/K; it means that a good thermoelectric performance of the Bi_2Te_3 crystal can maintain a broad temperature range. This is brought by a minor increment of the Te element in the directionally solidified crystal. The theoretical calculation results clearly revealed that the Seebeck coefficient reduces with the increase of temperature, matching well with the experimental data below 400 K. As the temperature surpasses 400 K, a deviation is apparently observed in Fig. 6. This may be attributed to the mixed n- and p-type conduction cancelling the induced Seebeck voltages out[20] and the strong interactions between charge carriers restricting their occupied states.[30]

3.2.3. Power factor (PF) and ZT

Figure 7 presents the relation of the power factor as a function of temperature in directionally solidified Bi_2Te_3 alloys at different growth rates. The measured PF values drop sharply with increasing temperature below 420 K. At $T >$ 420 K, the PF values decrease slightly for the Bi_2Te_3 crystals grown both at 3.5 mm/h and 18 mm/h. The optimum PF value of the n-type Bi_2Te_3 alloy solidified at 18 mm/h achieves 3.3×10^{-3} W/(K^2·m) at 300 K, which is larger than 3.1×10^{-3} W/(K^2·m) reported by Pichanusakorna *et al.*,[35] and 5 times larger than the p-type single Bi_2Te_3 crystal reported by Nassary *et al.*[14] At 520 K, the PF value of the Bi_2Te_3 crystal solidified at 18 mm/h can remain 1.6×10^{-3} W/(K^2·m), presenting good performance of the n-type thermoelectric material.

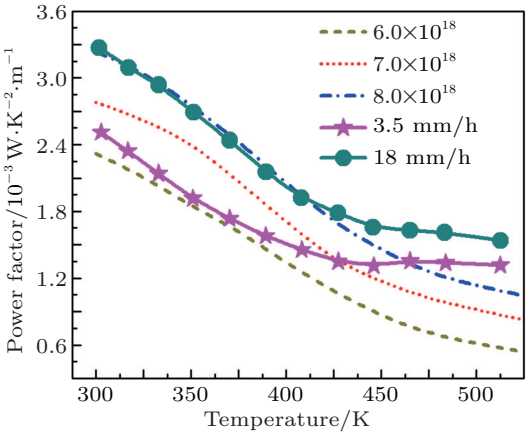


Fig. 7. (color online) Power factor (PF) as a function of temperature in directionally solidified Bi_2Te_3 alloys at different growth rates (solid lines) and theoretical calculations (dash lines).

The experimentally measured data of the Bi_2Te_3 crystal are within the scope of the theoretical computation as indicated in Fig. 7. The PF values of the crystal grown at 18 mm/h fit very well with the calculated results under the electronic concentration doping of 8.0×10^{18} cm^{-3} below 400 K. The PF value of the Bi_2Te_3 crystal directionally solidified at 18 mm/h is greater than that at 3.5 mm/h, because the PF, defined as $S^2\sigma$, mainly depends on the Seebeck coefficient, S, rather than the electrical conductivity, σ.

Similar to the power factor, the temperature dependence of the measured thermoelectric conductivity k and the lattice

thermal conductivity k_L for the Bi_2Te_3 crystals are shown in the inner part of Fig. 8. For all Bi_2Te_3 crystals, the thermal conductivity k is elevated with increasing temperature and the magnitude ranges from 1.38 to 2.81 W/mK. This increment may be attributed to the enhancement in ambi-polar thermal conductivity.[36,37] With increasing growth rate, the thermal conductivities are lifted due to the contribution of increasing carrier concentration to the thermal conductivity. To the electronic thermal conductivity, it is estimated using the Wiedemann–Franz equation, $k_{el} = L\sigma T$, where L is the Lorenz constant and equals 2.45×10^{-8} V^2/K^2.[38] The lattice thermal conductivity k_L can be obtained using $k_L = k - k_{el}$. Because a low electrical conductivity of the grown Bi_2Te_3 crystals results in lower electronic thermal conductivity, the lattice thermal conductivity, k_l, becomes the major part of the thermoelectric conductivity. It implies that the phonons that predominate the conduction of heat can hardly scatter in the crystals.[39,40]

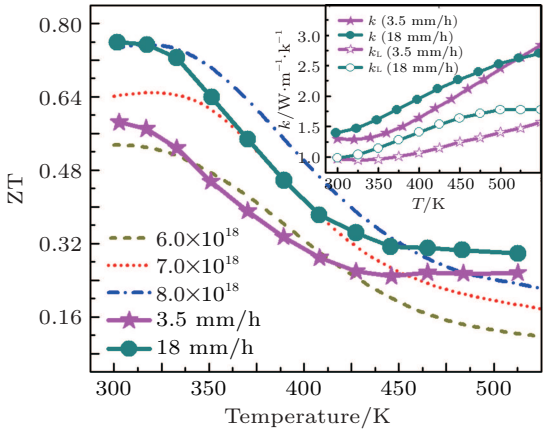


Fig. 8. (color online) ZT as a function of temperature in directionally solidified Bi_2Te_3 alloys at different growth rates (solid lines) and theoretical calculations (dash lines). Inset: the measured thermal conductivity k and lattice thermal conductivity k_L of the grown crystals at the rates of 3.5 mm/h and 18 mm/h.

According to the thermal conductivity, the figure of merit ZT, a key parameter to determine the performance of the thermoelectric material, can be calculated using ZT = PF/k. The obtained results are plotted in Fig. 8. The ZT of the crystal grown at 18 mm/h is greater than that at 3.5 mm/h. At 300 K, a maximum value of 0.74 was obtained for the crystal grown at 18 mm/h. At the growth rate of 3.5 mm/h, the ZT value can reach 0.6 for the crystal. As shown in Fig. 8, the theoretical calculation results of ZT match well with the experimental results except for the temperature above 400 K, similar to the electrical conductivity, Seebeck coefficient, and power factor shown in Figs. 5–7. The departure between the theoretical calculations and the experimental results at high temperatures is an open question, demanding further investigation in theoretical research work. Nevertheless, the theoretical predication is applicable for the crystal in a certain temperature range, from 300 K to 400 K in this study.

4. Conclusions

Under high-temperature gradients, the preferred orientation bulk Bi_2Te_3 single crystals with reallocated chemical composition were successfully prepared by a directional solidification method. The thermoelectric properties of the prepared crystals close to the limit of constitutional undercooling were measured from 300 K to 520 K. The results indicate that the cleavage plane of the grown Bi_2Te_3 crystals is parallel to the growth direction. The Te content in the crystal deviates from the stoichiometry of the crystal with increasing directional growth rate. The Bi_2Te_3 alloy grown at 18 mm/h presents a good thermoelectric performance. At 300 K, a maximum Seebeck coefficient and electrical conductivity achieve -245 μV/K and 5.6×10^4 S/m, respectively. An optimal PF achieves 3.3×10^{-3} W/(K^2·m), and the figure of merit ZT can be obtained as 0.74 at 300 K. These good thermoelectric properties can be attributed to the minor increased Te content that causes the change in the electronic concentration in the crystal. This can also be confirmed by the theoretical prediction based on the first-principle calculation.

Acknowledgments

The authors would like to thank Dr. Xu Lei for his suggests on our manuscript. They would also like to acknowledge the support from the Center for High Performance Computing of Northwestern Polytechnical University, China.

References

[1] Chen Y L, Analytis J G, Chu J H, Liu Z K, Mo S K, Qi X L, Zhang H J, Lu D H, Dai X, Fang Z, Zhang S C, Fisher I R, Hussain Z and Shen Z X 2009 *Science* **325** 178
[2] Hamdou B, Kimling J, Dorn A, Pippel E, Rostek R, Woias P and Nielsch K 2013 *Adv. Mater.* **25** 239
[3] Min Y, Roh J W, Yang H, Park M, Kim S, Hwang S, Lee S M, Lee K H and Jeong U 2013 *Adv. Mater.* **25** 1425
[4] Zhang H, Liu C X, Qi X L, Dai X, Fang Z and Zhang S C 2009 *Nat. Phys.* **5** 438
[5] Heinz N A, Ikeda T and Snyder G J 2012 *Acta Mater.* **60** 4461
[6] Wang G, Zhu X G, Sun Y Y, *et al.* 2011 *Adv. Mater.* 2929
[7] Rowe D M 1995 *CRC Handbook of Thermoelectrics* (Boca Raton, Florida: CRC press) pp. 216–218
[8] Nolas G S, Sharp J and Goldsmid J 2001 *Thermoelectrics: Basic Principles and New Materials Developments* (Berlin: Springer) pp. 59–87
[9] Cosgrove G J, McHugh J P and Tiller W A 1961 *J. Appl. Phys.* **32** 621
[10] Shen J J, Hu L P, Zhu T J and Zhao X B 2011 *Appl. Phys. Lett.* **99** 124102
[11] Kim D H, Kim C, Heo S H and Kim H Y 2011 *Acta Mater.* **59** 405
[12] Ni H L, Zhu T J and Zhao X B 2005 *Mater. Sci. Eng. B* **117** 119
[13] Miura S, Sato Y, Fukuda K, Nishimura K and Ikeda K 2000 *Mater. Sci. Eng. A* **277** 244
[14] Nassary M M, Shaban H T and El-Sadek M S 2009 *Mater. Chem. Phys.* **113** 385
[15] Yamashita O and Tomiyoshi S 2003 *J. Appl. Phys.* **93** 368
[16] Zou H L, Rowe D M and Min G 2001 *J. Cryst. Growth* **222** 82
[17] Ha H P, Hyun D B, Byun J Y and Oh Y J 2002 *J. Appl. Phys.* **37** 4691
[18] Feng S K, Li S M, Luo Q Y and Fu H Z 2011 *Adv. Mater. Res.* **197** 1109
[19] Fleurial J P, Gailliard L, Triboulet R, Scherrer H and Scherrer S 1988 *J. Phys. Chem. Solids* **49** 1237
[20] Snyder G J and Toberer E S 2008 *Nat. Mater.* **7** 105

[21] Paolo G, Stefano B, Nicola B, *et al*. 2009 *J. Phys.: Condens. Matter* **21** 395502
[22] Perdew J P, Burke K and Ernzerhof M 1996 *Phys. Rev. Lett.* **77** 3865
[23] Vanderbilt D 1990 *Phys. Rev. B* **41** 7892
[24] Liu D C and Nocedal J 1989 *Math. Program.* **45** 503
[25] Madsen G K H and Singh D J 2006 *Comput. Phys. Commun.* **175** 67
[26] Dantzig J A and Rappaz M 2009 *Solidification* (Switzerland: EPFL Press) p. 305
[27] Chitroub M, Scherrer S and Scherrer H 2000 *J. Phys. Chem. Solid.* **61** 1693
[28] Ainsworth L 1956 *P. Phys. Soc. B* **69** 606
[29] Stefanescu D M 2008 *Science and Engineering of Casting Solidification* (New York: Springer) p. 137
[30] Scherrer H and Scherrer S 2006 *Thermoelectrics Handbook: Macro to Nano* (CRC Press: Taylor & Francis Group) p. 16
[31] Stern F 1980 *Phys. Rev. Lett.* **44** 1469
[32] Vining C B 1991 *J. Appl. Phys.* **69** 331
[33] Sootsman J R, Kong H J, Uher C, D'Angelo J J, Wu C I, Hogan T P, Caillat T and Kanatzidis M G 2008 *Angew. Chem.* **120** 8746
[34] Ramu A T, Cassels L E, Hackman N H, Lu H, Zide J M O and Bowers J E 2010 *J. Appl. Phys.* **107** 083707
[35] Pichanusakorn P and Bandaru P R 2009 *Appl. Phys. Lett.* **94** 223108
[36] Wang S Y, Tan G J, Xie W J, Zheng G, Li H, Yang J H and Tang X F 2012 *J. Mater. Chem.* **22** 20943
[37] Satterthwaite C B and Ure R W 1957 *Phy. Rev.* **108** 1164
[38] Takashiri M, Miyazaki K, Tanaka S, Kurosaki J, Nagai D and Tsukamoto H 2008 *J. Appl. Phys.* **104** 084302
[39] Chernatynskiy A and Phillpot S R 2013 *Curr. Opin. Solid State Mater. Sci.* **17** 1
[40] Qiu B and Ruan X L 2009 *Phys. Rev. B* **80** 165203